



Research Article

The impact of thermal stratification and heat generation/absorption on MHD Carreau nano fluid flow over a permeable cylinder

D. Gopal¹ · S. Hari Shing Naik¹ · N. Kishan¹ · C. S. K. Raju² 

Received: 22 January 2020 / Accepted: 6 March 2020 / Published online: 13 March 2020
© Springer Nature Switzerland AG 2020

Abstract

The impact of magnetic field, nanoparticles on the two-dimensional flow of a generalized non-Newtonian Carreau fluid flow over a permeable cylindrical surface with no slip condition has been investigated in the existence of heat generation/absorption, thermal stratification and thermal radiation. The mentioned sets of nonlinear governing differential equations are converted into nonlinear ordinary differential equations by using appropriate similarity transformations and solved numerically and find with shooting technique performed in this concern. It is initiate that the two various values of magnetic parameter (M), heat generation/absorption parameter (H) and power law index (n) influences velocity, temperature and nanoparticle volume fraction profiles. Finally, in this article the impact of various parameters on skin friction coefficient, Nusselt number and Sherwood numbers are examined with the support of the tabular form.

Keywords Thermal radiation · Heat generation/absorption · MHD · Carreau fluid · Thermal stratification

1 Introduction

The investigation of non-Newtonian fluids is extensive subject of extreme interest for the scientists and experts. The non-Newtonian fluid is defined as the nonlinear relations between shear rate and shear stress. The non-Newtonian fluids are most regularly used in blood, printing colours and inks, greasing oils and Greases, toothpaste, shampoos, nail polish, cosmetics, and creams and lotions, shaving suds, snacks, combination of cake and coatings cake, white egg, dressings salad, jams, bread amalgams various molten polymers are to mention just a few with daily life concern. Various novelists examine different kinds of non-Newtonian fluid models are deliberating their flow in the direction of different surfaces in an occurrence of an appropriate physical effects. The historical and latest developments in this direction can be assessed in Refs. [1–5]. The materials specifically melting proteins and

polymers, suds, solid creams, waxy oils, polymers solution, crudes oil, pharmaceuticals reproduces the thinning of shear characteristics. For such kinds of non-Newtonian fluid constituents, the influence of viscosity is initiate to be an occupation of shear rate and can be designated by an appropriate fluid model similar to Carreau fluid models [6, 7]. Three-dimensional flow of Casson–Carreau fluids stretching surface model deliberated by Raju et al. and Gireesha et al. [8, 9]. The stratification model an appropriate to the period of non-Newtonian fluid model is deliberated by investigators [10–15], here Carreau fluid model delivers enhanced estimates for many shear thinning fluids for the constitutive association of Carreau fluid model grips at both lower and higher shear rates.

The property of Magneto hydrodynamic (MHD) is the electrically magnifying the fluids, and then a conductor transporting electrical energy exchanges into a magnetic field. Magneto hydrodynamic (MHD) has numerous

✉ C. S. K. Raju, sivaphd90@gmail.com; D. Gopal, degavath.gopal@gmail.com; S. Hari Shing Naik, shnr10@yahoo.com; N. Kishan, kishan.naikoti@gmail.com | ¹Department of Mathematics, UCS, Osmania University, Hyderabad, India. ²Department of Mathematics, GITAM School of Science, GITAM University, Bangalore 562163, India.



significances in magnetic sensors, cosmology, astrophysics, and geophysics, drugs, engineering and solid. The impact of heat transfer in terms of thermal radiation and MHD assume a noteworthy part in industry especially in assembling and industrial equipment's that incorporate rockets, space vehicles, gas turbines, satellites, nuclear plants and many others. So many researchers studied on MHD Carreau fluid flow [16–20]. The stratification impact on magneto hydrodynamics fluid flow is founded in the poetry as yet particularly when fluid flow is encouraged by stretching cylindrical surface are discoursed Khalil et al. [21], Mixed Convection Stagnation-Point Flow on MHD discussed by Madhu et al. [22], heat transfer over stretching sheet variable viscous dissipation and heat source/sink on MHD has deliberated by Dessie [23]. Non-Newtonian power-law fluids flowing over a wedge with heat source/sink in presence of viscous dissipation deliberated by Kishan et al. [24], Here, the uniqueness of current effort is to study the velocity, temperature nanofluid stratification enforced in the fluid flow system of magneto hydrodynamic (MHD) Carreau fluid flow models. Recently, the various investigators [25–36] are considered magneto hydrodynamic with the various flow configurations (disk, stretched surface, cylinder, symmetric and asymmetric flow) and various physical parameters (suction, Multiwall carbon nanotubes, nanoparticles, non-Fourier heat flux). With their studies highlighted that the non-Newtonian fluid has tendency to control the flow performance.

The ignoring on overwhelming standing of generation/absorption reactions on MHD Carreau fluid flow with thermally stratified and the boundary layer flow of MHD Carreau fluid over a permeable cylinder. The major objective of this work is to scrutinize the impacts of generation/absorption and thermally reactions on MHD Carreau fluid flow over a linearly permeable cylinder under the inspiration of functional magnetic field. The fluid flow of governing equations is numerically attempted with shooting technique. The consequence of governing physical parameters are interested quantities (velocity, temperature, nanofluid, skin friction, Nusselt and Sherwood numbers) are specified through graphical and tabular illustrations.

2 Mathematical formulation

The steady 2-dimensional boundary layer flow of incompressible thermally stratified Carreau fluid flow over a permeable stretching cylinder surface has been deliberated. The coordinate system is elected in such a method

that x -axis is restrained along with the stretching cylinder though r -axis. The magnetic field (B_0) is identical and functional in r -direction and the encouraged magnetic field is under small Reynolds magnetic number. The stretching cylinder velocity is supposed to be $u_w = U_0 x L^{-1}$ where $U_0 > 0$, and L is the specific length. The surface temperature of the cylinder is $T_w(x) = T_0 + bxL^{-1}$, where b is arbitrary constant and T_0 is the free stream temperature. Here, Carreau fluid flow has been expected alongside x -direction and r -direction is measured perpendicular to fluid flow.

Also taking the two dimensional cylindrical steady flow, velocity, temperature, nanoparticle volume friction are theoretical to be the form of:

$$V = [u = (x, r); v = (x, r)], T = T(x, r), C = C(x, r) \tag{1}$$

Here, u and v denotes the velocity variable in x - and r -direction. The convective model transport designed for the Carreau fluid flow model is governing by the equations of mass, momentum, energy and concentration are followed as [16]:

$$(ru)_x + (rv)_r = 0 \tag{2}$$

$$u(u_x) + v(u_r) = v' \left[u_{rr} + r^{-1}u_r + \frac{3\Gamma^2(n-1)}{2}(u_r)^2(u_{rr}) + \frac{3\Gamma^2r^{-1}(n-1)}{2}(u_r)^3 \right] - \sigma B_0^2 \rho^{-1}u \tag{3}$$

$$u(T_x) + v(T_r) = \alpha' [T_{rr} + r^{-1}T_r] + \tau^* [D_B C_r T_r + D_T (T_r)^2] + Q_0(\rho c p)^{-1}(T - T_\infty) \tag{4}$$

$$u(C_x) + v(C_r) = D_B [C_{rr} + r^{-1}C_r] + D_T T_\infty^{-1} T_{rr} \tag{5}$$

In above equations u and v are the velocity components. These components are parallel to x and r directions correspondingly. Here kinematic viscosity is v' , the electrical conductivity of the fluid is σ , the coefficient of thermal expansion is β_T , the gravity is g , the fluid density is ρ_f , the fluid temperature is T , the temperature of the ambient fluid is T_∞ , the coefficient of expansion with concentration is β_C , the fluid concentration is C and the nanoparticle concentration C_∞ is far away from the surface, the thermal diffusivity is α' , the effective heat capacity of the nanoparticle is $(\rho c)_p$ and the effective heat capacity of fluid is $(\rho c)_f$, the Brownian diffusion coefficient is D_B , the thermophoresis diffusion coefficient is D_T , the specific heat capacity is c_p , the volumetric heat generation/absorption is Q_0 .

Also, the boundary condition are given below:

$$\begin{aligned}
 u(x, r) &= U_0 L^{-1} x, \quad v(x, r) = 0, \quad T(x, r) = T_w \\
 (x) &= T_0 + b x L^{-1}, \quad C = C_w(x) \text{ at } r = R \\
 u(x, r) &\rightarrow 0, \quad v(x, r) \rightarrow 0, \quad T(x, r) \rightarrow T_\infty \\
 (x) &= T_0 + c x L^{-1}, \quad C(x, r) = C_\infty(x) \text{ as } r \rightarrow \infty
 \end{aligned} \tag{6}$$

The velocity components in terms of stream function ψ can be written by form

$$u(x, r) = r^{-1}(\psi_r), \quad v = -r^{-1}(\psi_x)$$

Where ψ_r, ψ_x are differentiation with respect to r, x and similarity variables are

$$\begin{aligned}
 u &= U_0 x L^{-1} F'(\zeta), \quad v = -R r^{-1} [U_0 v^* L^{-1}]^{0.5}, \\
 \zeta &= (2R)^{-1} [r^2 - R^2 (U_0 (v^* L)^{-1})^{-0.5}], \\
 \psi &= [U_0 v^* x^2 L^{-1}]^{-0.5}, \quad (T_w - T_0) T(\zeta) = T - T_\infty, \\
 (C_w - C_0) C(\zeta) &= C - C_\infty
 \end{aligned} \tag{7}$$

The above governing Eqs. (2)–(5) are transformed as follows,

$$\begin{aligned}
 (1 + 2K_\zeta) F_{\zeta\zeta\zeta}(\zeta) &\left[1 + \frac{3}{2}(n-1)\lambda^2(1 + 2K_\zeta)(F_{\zeta\zeta}(\zeta))^2 \right] \\
 + K F_{\zeta\zeta}(\zeta) &\left[1 + (1 + 2K_\zeta) \frac{n-1}{2} \lambda^2 F_{\zeta\zeta}^2 \right] \\
 + F(\zeta) F_{\zeta\zeta}(\zeta) - F_\zeta(\zeta)^2 - M F_\zeta(\zeta) &= 0
 \end{aligned} \tag{8}$$

$$\begin{aligned}
 (1 + 2K_\zeta) T_{\zeta\zeta}(\zeta) + K T_\zeta + \text{Pr}(1 + 2K_\zeta) [N b T(\zeta) C_\zeta(\zeta) \\
 + N t T_\zeta(\zeta)^2] + F(\zeta) T_\zeta(\zeta) + H T(\zeta) &= 0
 \end{aligned} \tag{9}$$

$$(1 + 2K_\zeta) C_{\zeta\zeta}(\zeta) + K C_\zeta(\zeta) + \text{Le Pr } F(\zeta) C_\zeta(\zeta) + (1 + 2K_\zeta) \frac{N t}{N b} T_{\zeta\zeta}(\zeta) = 0 \tag{10}$$

The non-dimensional form of the boundary conditions are,

$$\begin{aligned}
 F(\zeta) = 0, \quad F_\zeta(\zeta) = 1, \quad T(\zeta) = 1 - k_1, \quad C(\zeta) = 1, \quad \text{as } \zeta \rightarrow 0 \\
 F_\zeta(\zeta) \rightarrow 0, \quad T(\zeta) \rightarrow 0, \quad C(\zeta) \rightarrow 0 \text{ at } \zeta \rightarrow \infty
 \end{aligned} \tag{11}$$

In above equation, F_ζ denotes differentiation with respect to ζ . The non-dimensional parameters defined as:

Where some of non-dimensional parameters associated as, n is power law index, the curvature parameter is $K \left(= \frac{1}{R} \sqrt{\frac{L v^*}{U_0}} \right)$, the thermal stratification parameter is $k_1 \left(= \frac{\zeta}{b} \right)$, the Weissenberg number is $\lambda \left(= \Gamma \sqrt{\frac{U_0^2}{L^2 v^* x}} \right)$, the

magnetic parameter is $M \left(= \frac{2\sigma B_0^2}{\rho_f(n+1)} \right)$, the Prandtl number is $\text{Pr} (= v/\alpha)$, the Brownian motion parameter is $Nb \left(= \frac{(\rho c)_p D_B (C_w - C_\infty)}{v(\rho c)_f} \right)$, the thermophoresis parameter is $Nt \left(= \frac{(\rho c)_p D_T (T_w - T_\infty)}{v(\rho c)_f T_\infty} \right)$, and the heat generation/absorption coefficient is $H \left(= \frac{2x Q_0}{(\rho c)_f(n+1) U_w} \right)$.

For engineering concerned, physical parameters are the skin friction coefficient C_{f_x} , local Nusselt number Nu_x and local Sherwood number Sh_x given as,

$$\begin{aligned}
 C_F &= \frac{T_w}{\rho U_w^2} \text{ where } \tau_w = \mu \left[u_r + \frac{\Gamma^2(n-1)}{\sqrt{2}} (u_r)^3 \right]_{r=R}, \\
 Nu_x &= \frac{x q_w}{k(T_w - T_0)} \text{ where } q_w = -k(T_r)_{r=R}, \\
 Sh_x &= \frac{x q_m}{D_B(C_w - C_0)} \text{ where } q_m = -D_m(C_r)_{r=R}.
 \end{aligned} \tag{12}$$

Ultimately by introducing Eq. (7) the above Eq. (12) is converting into surface drag force, heat transfer and mass transfer rates are

$$\begin{aligned}
 \text{Re}_x^{0.5} C_F &= F_{\zeta\zeta}(0) + \frac{\lambda^2(n-1)}{2} (F_{\zeta\zeta}(0))^3, \\
 \text{Re}_x^{-0.5} Nu_x &= -T_\zeta(0), \quad \text{Re}_x^{-0.5} Sh_x = -C_\zeta(0) \\
 \text{Re}_x &= \frac{x U_0 x^2}{v^* L} \text{ is shows that Reynolds number.}
 \end{aligned}$$

3 Numerical solution

In this section, the governing Eqs. (8)–(10) with boundary condition (11) are reduced to IVP by decreasing the higher order into first order with using dummy substitution is achieved as follows

$$\begin{pmatrix} u_1 \\ u_2 \\ u_3 \\ u_4 \\ u_5 \\ u_6 \\ u_7 \end{pmatrix} = \begin{pmatrix} F(\zeta) \\ (u_1) = F_\zeta(\zeta) \\ (u_2)_\zeta = (u_1)_{\zeta\zeta} = F_{\zeta\zeta}(\zeta) \\ T(\zeta) \\ (u_4)_\zeta = T_\zeta(\zeta) \\ C(\zeta) \\ (u_6)_\zeta = C_\zeta(\zeta) \end{pmatrix}$$

Replace the above given equation are the governing equations and boundary conditions (8)–(11) are solved by numerically via shooting method. Additionally, it is important to select a finite value of ζ_∞ . The higher order equations converted as follows

and Nanofluid concentration $C(\zeta)$ profiles are displayed through graphs. The variation in the velocity, temperature, nanoparticle volume fraction profiles for different values of Weissenberg number ($\lambda = 1.2, 1.4, 1.6$) for both the power law index of values at $n < 1$ shear thinning

$$\begin{pmatrix} (u_1)_\zeta \\ (u_2)_\zeta \\ (u_3)_\zeta \\ (u_4)_\zeta \\ (u_5)_\zeta \\ (u_6)_\zeta \\ (u_7)_\zeta \end{pmatrix} = \begin{pmatrix} u_2 \\ u_3 \\ \frac{(u_2)^2 + Mu_2 - u_1u_3 - Ku_3[1 + (n-1)/2(1+2K\zeta)\lambda^2u_3^2]}{(1+2K\zeta)(1+1.5(n-1)\lambda^2(1+2K\zeta)u_3^2)} \\ u_5 \\ -\frac{Ku_5 + Pr(1+2K\zeta)(Nbu_4u_7 + Ntu_5^2 + u_1u_5 + Hu_4)}{(1+2K\zeta)} \\ u_6 \\ -\frac{Ku_7 + LePr u_1u_7 + (Nt/Nb)(1+2K\zeta)u_5}{(1+2K\zeta)} \end{pmatrix}$$

In the above $(u_r)_\zeta$, $r = 1$ to 7 denotes differentiation with respect to ζ . The converted boundary conditions in relation of one point conditions are written below

$$u_1(0) = 0, u_2(0) = 1, u_3(0) = h_1, u_4(0) = 1 - k_1, \\ u_5(0) = h_2, u_6(0) = 1, u_7(0) = h_3.$$

The outline field condition are converted as $u_2(\infty) = 0, u_4(\infty) = 0, u_6(\infty) = 0$ where h_1, h_2 and h_3 are primary used on the performance of computational algorithm.

4 Results and discussion

For the observation results in the current study a numerical computation is achieved for the impact of heat generation/absorption and thermally stratified on MHD Carreau nanofluid on a permeable cylinder. The non-linear coupled governing Eqs. (8)–(10) and the equivalent boundary condition Eq. (11) are achieved by numerically applying shooting technique. Additionally, characteristic outcomes of skin friction (C_f), Nusselt number (Nu) and Sherwood number (Sh) are chronicled with the tables. The various non-dimensional identical parameters $\lambda, M, n, H^+, H^-, Nb, Nt, K, Pr, Le$ on the flow, dimensionless fluid velocity $F'(\zeta)$, temperature $T(\zeta)$

and $n > 1$ shear thickening cases, as it is noticed from the figures that the shear thinning flow case has lesser than the shear thickening flow case. Figures 1, 2 and 3 display that the velocity, temperature, nanoparticle volume fraction profiles have a thickness of thermal boundary layers moderate with enriching values of Weissenberg number in both cases of shear thickening and shear thinning fluids. Here, we found that the higher variations in the velocity, temperature, nanoparticle volume fraction for improved values of Weissenberg number, whereas the temperature, nanoparticle volume fraction profiles are boosting with boosting of Weissenberg number and velocity decreases.

Figure 4 shows the performance of the velocity profile for several values of physical parameters. Limitations of curvature parameter and buoyancy forces are floating body in cylinder flow has two different value of magnetic parameter. In this figure curvature parameter ($K = 1.3, 1.6, 1.9$) values are boosting then the velocity profile declining, the impression of buoyancy parameter has moreover controlling than the curvature parameter. Figure 5 exposes that impression of magnetic field parameter (M) on nanoparticle volume fraction $C(\zeta)$ profiles for two specific changed flows of power law index at $n < 1$ it shear thinning and $n > 1$ it shear thickening respected the circulation, at shear thinning flow case is reduces then the shear thickening flow cases. The clear improvement of magnetic parameter

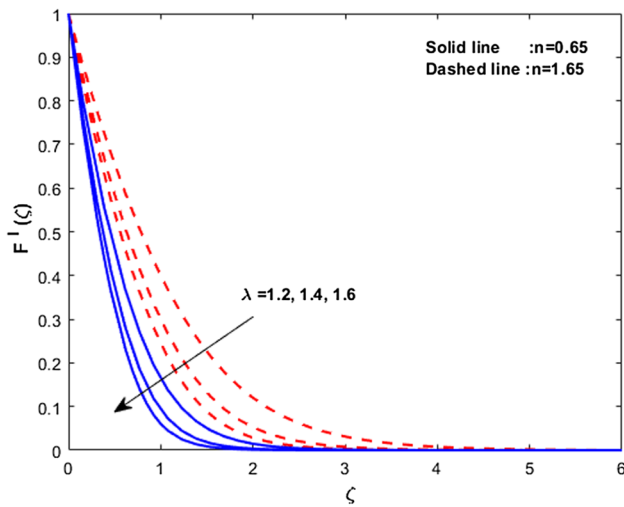


Fig. 1 Influence of Weissenberg number (λ) on velocity profile ($F'(\zeta)$)

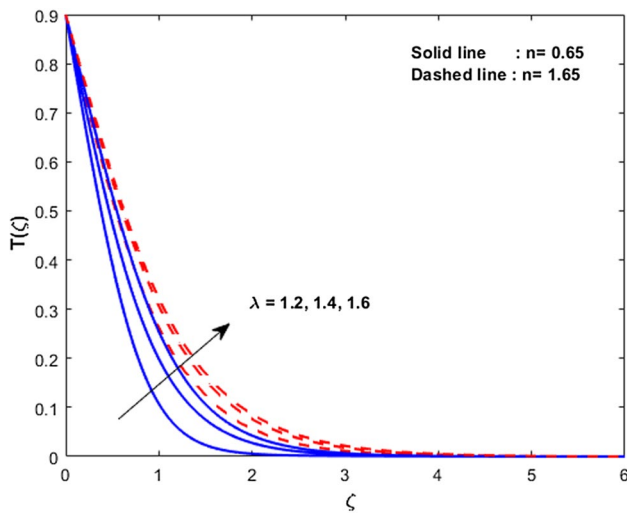


Fig. 2 Influence of Weissenberg number (λ) on temperature profile ($T(\zeta)$)

($M = 1.0, 3.0, 5.0$) enhancing nanoparticle volume friction profile due to the impeding force on the flow and rising on magnetic parameter M increase Lorentz force produced by magnetic field, thus degeneration struggle to the nanoparticle fluid flow.

Figure 6 shows the impact of Brownian motion parameter (Nb) on velocity profile for two cases of generation and absorption flows. The influence of Brownian motion

is higher in heat generation case compared with heat absorption case. Moreover, the boosting values of Brownian motion ($Nb = 1.1, 1.3, 1.5$) enhanced the velocity profile in both the heat generation and absorption flow cases. Figure 7, expresses the concentration profiles in the presence of Brownian motion for both the magnetic and without magnetic field cases. The concentration profiles are reduced with improvement in the Brownian motion. Figures 8, 9 and 10 demonstrate that the various values of thermophoresis parameters ($Nt = 1, 2, 3$) affecting velocity, temperature and nanoparticle volume fraction profiles due to the two cases of generation and absorption flows. Here having higher kinetic energy with their higher velocity, temperature and nanoparticle volume friction. When they strike with the large, slow moving particles of the nanofluid they push the latter away from the boundary layer. The force that has pushed the nanoparticles away from the boundary is thermophoretic force. Due to this force enhancing the velocity and nanoparticle volume fraction whereas declines the temperature profile.

Figure 11 shows the effects of the Prandtl number (Pr) on the temperature profile $T(\zeta)$ for the two cases of heat generation and heat absorption. Also, we observed here the heat generation flow has higher thermal boundary layers thickness is compared to heat absorption flow cases. Moreover rising values of ($Pr = 2.2, 2.4, 2.6$) reduces the temperature profile. That is the small Prandtl number (Pr) shows fluids with high thermal conductivity and this creates thicker thermal boundary layer structures of large Prandtl number. Figures 12 and 13 show the consequence of Lewis number on the temperature profile, nano fluid profiles established on the heat transfer of the external flow at generation and absorption in cylindrical flow. As depicts in Fig. 12, the temperature rising very speedily and spread for small Lewis Number ($Le = 0.5, 1.0, 1.5$) conversely, with Lewis number boosting. The Lewis number influence on the nanoparticle volume friction profile on the convective heat transfer inside the cylinder has been shown in Fig. 13, the nanoparticle volume friction profile declines radically at the arrival region of fully established cylinder area when boosting values of Lewis number.

Tables 1, 2 and 3 displays the effects of various active physical parameters on skin fraction, Nusselt number and Sherwood numbers for with curvature and without curvature cases. From these Tables, we found that the rate of heat transfer is increased with the thermophoresis and reduced with the Brownian motion as well as heat generation parameters; these are displayed in Table 2. Here, it is

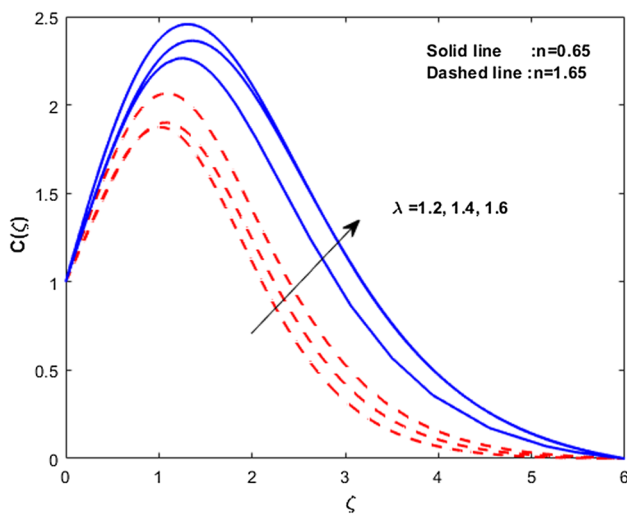


Fig. 3 Influence of Weissenberg number (λ) on nano particle volume fraction profile ($C(\zeta)$)

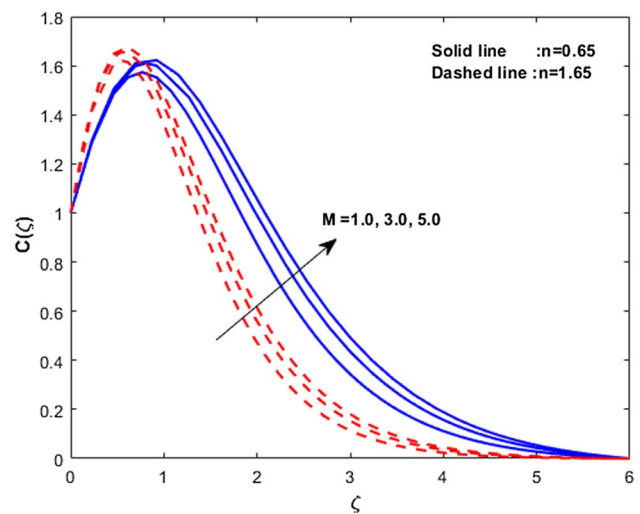


Fig. 5 Influence of magnetic parameter (M) on nano particle volume fraction profile ($C(\zeta)$)

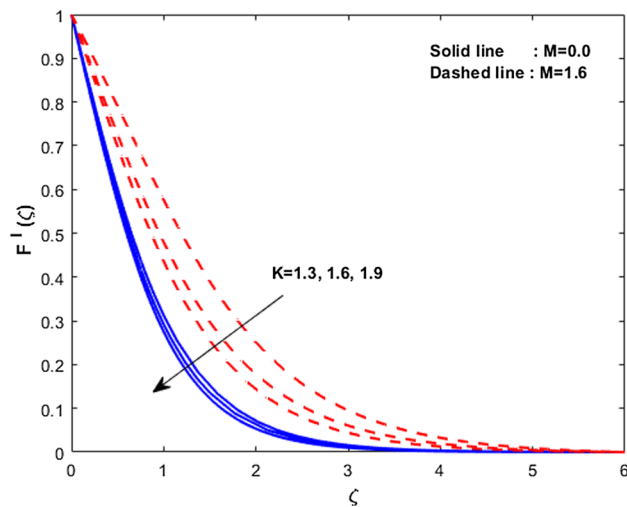


Fig. 4 Influence of curvature parameter (K) on velocity profile ($F'(\zeta)$)

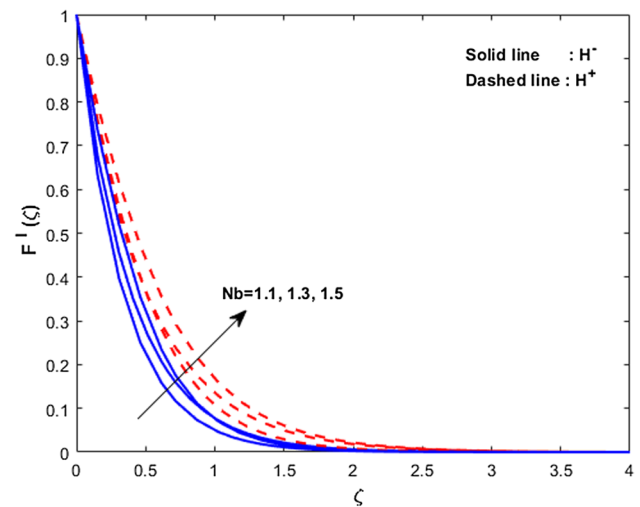


Fig. 6 Influence of Brownian motion (Nb) on velocity profile ($F'(\zeta)$)

interesting to mention that the friction at the wall, mass transfer rate and heat transfer rate are higher in the inclusion of curvature parameter compared to without curvature parameter. Table 1 depicts the skin friction coefficient on improving values of various physical parameters n, M, λ . The Skin friction coefficient has enhanced with M and decline with n, λ . Table 3 signifies the impact of k_1, Pr, Le on Sherwood number of curvature and without curvature in both the cases. Interestingly, we found that the Sherwood number is improved for all the parameters (Thermal Stratification, Lewis and Prandtl number).

5 Conclusion

In the present study deals with the effects of heat generation/absorption and thermal stratification on MHD Carreau nanofluid on permeable cylinder. The arising sets of nonlinear governing differential equations are converted into nonlinear ordinary differential equations with aid of appropriate similarity transformations and solved numerically. For significance of engineering interest, we also calculated the C_f, Nu and Sh . The following specified deductions are

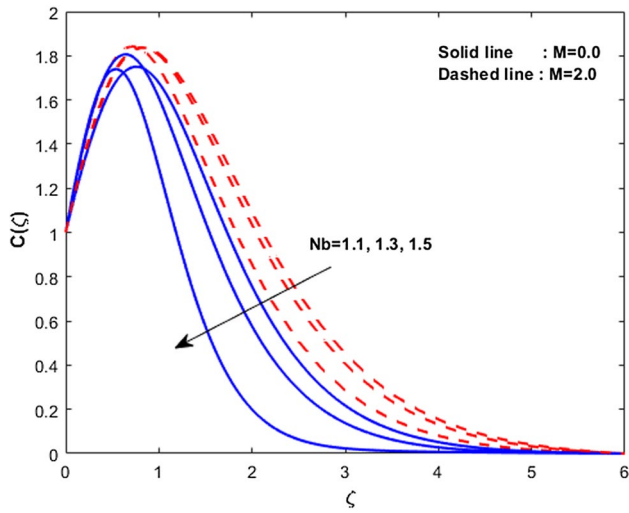


Fig. 7 Influence of Brownian motion (Nb) on nano particle volume fraction profile ($C(\zeta)$)

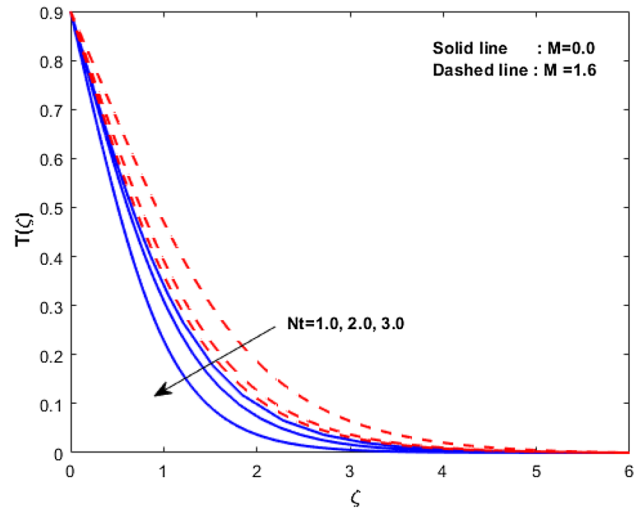


Fig. 9 Influence of thermophoresis parameter (Nt) on temperature profile ($T(\zeta)$)

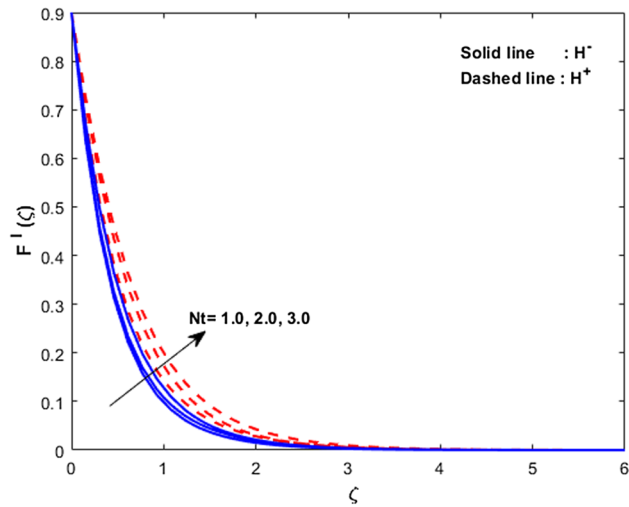


Fig. 8 Influence of thermophoresis parameter (Nt) on velocity profile ($F'(\zeta)$)

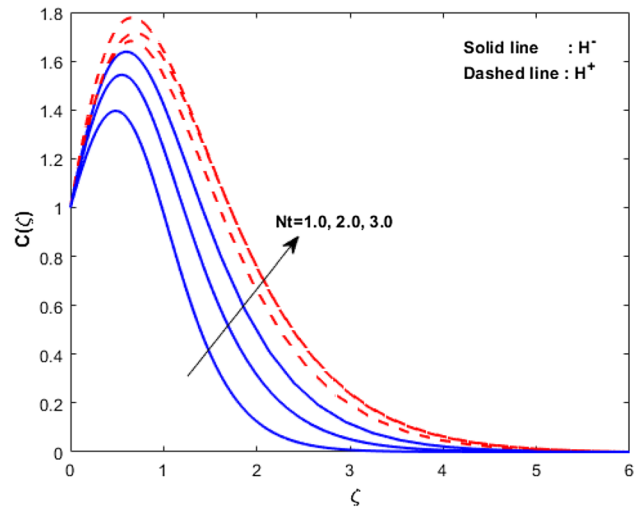


Fig. 10 Influence of thermophoresis parameter (Nt) on nano particle volume fraction profile ($C(\zeta)$)

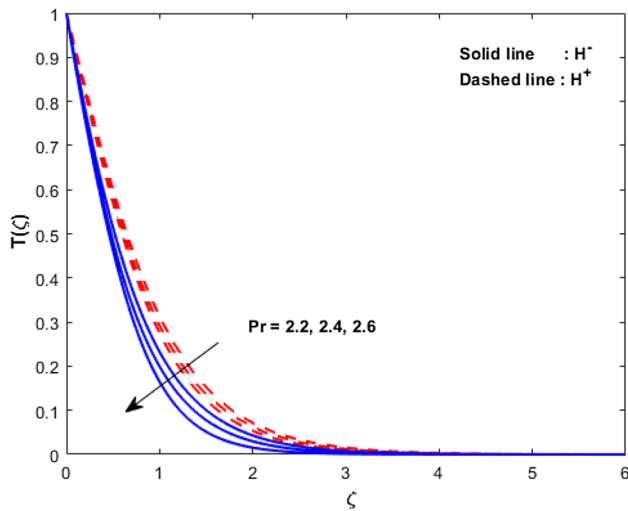


Fig. 11 Influence of Prandtl number (Pr) on temperature profile ($T(\zeta)$)

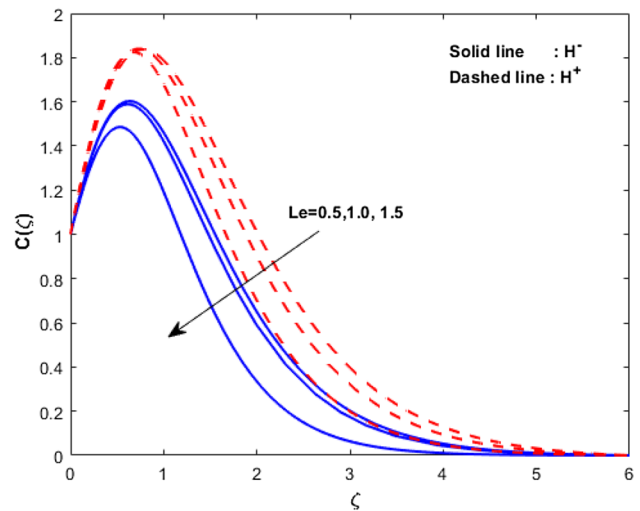


Fig. 13 Influence of Lewis number (Le) on nano particle volume fraction profile ($C(\zeta)$)

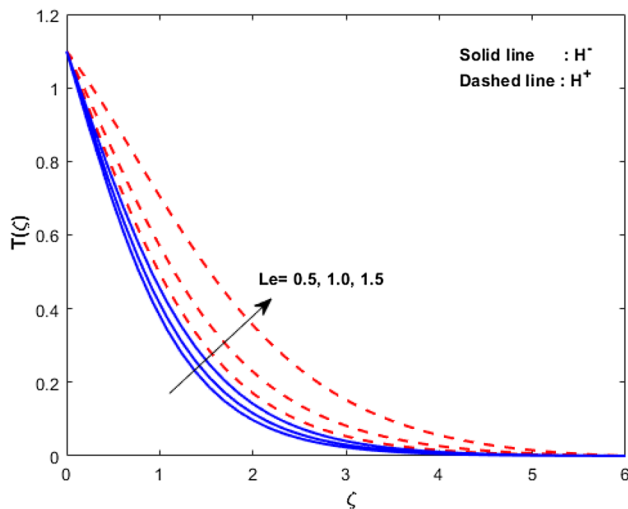


Fig. 12 Influence of Lewis number (Le) on temperature profile ($T(\zeta)$)

Table 1 The modulation of skin friction for n, M, λ at $Nb = 0.3, Nt = 0.2, k_1 = 0.2, Pr = 0.72, Le = 0.4$.

n	M	λ	$Re^{0.5} C_f$ cylinder ($K = 1.0$)	$Re^{0.5} C_f$ Sheet ($K = 0.0$)
1.2	1.5	2.0	-0.173841	-1.269133
2.2	1.5	2.0	-0.413874	-1.410210
3.2	1.5	2.0	-0.707880	-1.502896
1.0	1.0	1.0	-0.595455	-1.854190
1.0	3.0	3.0	-0.319459	-1.845262
1.0	5.0	5.0	-0.139812	-1.803797
1.0	1.5	0.5	-0.525855	-1.844190
1.0	1.5	1.0	-0.526514	-1.844636
1.0	1.5	1.5	-0.527523	-1.844849

- The Lewis number and Thermal Stratification parameters are improves the Sherwood number for both the curvature and without curvature. It is also interesting to mention that the mass transfer rate is higher in the presence of curvature compared without curvature.
- The Friction factor is more in the presence of curvature when compared to without curvature parameters. It clearly tells us that when we need more friction we can incorporate the curvature parameter in the flow.
- The influence of Brownian motion is higher in nanoparticle volume fraction in the presence of magnetic field compared to without magnetic field.

Table 2 The influence of Nusselt number for Nt, Nb, k_1 at $M = 0.6, n = 0.1, \lambda = 0.2, Pr = 0.72, Le = 0.4$.

Nt	Nb	H^+	$Re_x^{-0.5} Nu$ Cylinder ($K = 1.0$)	$Re_x^{-0.5} Nu$ Sheet ($K = 0.0$)
1.3	0.2	2.0	1.361249	0.794353
2.3			1.724936	1.060690
3.3			2.029857	1.280046
	1.5		0.553700	0.356561
	2.5		0.411697	0.320961
	3.5		0.377735	0.310794
		0.1	1.337940	0.677142
		0.2	1.292799	0.618645
		0.3	1.244857	0.554663

Table 3 The variation on Sherwood number for Nb , Nt , H^+ at $Nt = 0.2$, $Nb = 0.3$, $k_1 = 0.2$, $M = 0.6$, $n = 0.1$, $\lambda = 0.2$.

k_1	Pr	$LeRe_x^{-0.5}Sh$	$Re_x^{-0.5}Sh$	
			Cylinder ($K = 1.0$)	SHEET ($K = 0.0$)
0.2	0.2	2.0	1.227381	0.644227
0.4			1.275622	0.659894
0.6			1.325812	0.676486
	0.4		1.042592	0.404851
	0.6		1.091991	0.451330
	0.8		1.140290	0.498891
		1.0	1.187464	0.547106
		2.0	1.424093	0.802526
		3.0	1.635579	1.038473

- The heat generation has higher temperature boundary compared to heat absorption case. This helps to conclude the heat absorption is useful in cooling systems.

Compliance with ethical standards

Conflict of interest The authors declare that they have no conflict of interest.

References

- Hazem Ali Attia (2007) Investigation of non-Newtonian micropolar fluid flow with uniform suction/blowing and heat generation. *Turk J Eng Environ Sci* 30(6):359–365
- Yilmaz N, Bakhtiyarov AS, Ibragimov RN (2006) Experimental investigation of Newtonian and non-Newtonian fluid flows in porous media. *Mech Res Commun* 36(5):638–641
- Keimanesh M, Rashidi MM, Chamkha AJ, Jafari R (2011) Study of a third grade non-Newtonian fluid flow between two parallel plates using the multi-step differential transform method. *Comput Math Appl* 62(8):2871–2891
- Shojaeian M, Koşar A (2014) Convective heat transfer and entropy generation analysis on Newtonian and non-Newtonian fluid flows between parallel-plates under slip boundary conditions. *Int J Heat Mass Transf* 70:664–673
- Rehman K, Khan AA, Malik MY, Makinde OD (2017) Thermophysical aspects of stagnation point magnetonano fluid flow yields by an inclined stretching cylindrical surface: a non-Newtonian fluid model. *J Braz Soc Mech Sci Eng* 39(9):3669–3682
- Waqas M, Khan MI, Hayat T, Alsaedi A (2017) Numerical simulation for magneto Carreau nanofluid model with thermal radiation: a revised model. *Comput Meth Appl Mech Eng* 324:640–653
- Khellaf K, Lauriat G (2000) Numerical study of heat transfer in a non-Newtonian Carreau fluid between rotating concentric vertical cylinders. *J Non-Newtonian Fluid Mech* 89:45–61
- Raju CSK, Sandeep N (2016) Unsteady three-dimensional flow of Casson-Carreau fluids past a stretching surface. *Alex Eng J* 55(2):1115–1126
- Gireesha BJ, Sampath Kumar PB, Mahanthesh B, Shehzad SA, Rauf A (2017) Nonlinear 3D flow of Casson–Carreau fluids with homogeneous–heterogeneous reactions: a comparative study. *Results Phys* 7:2762–2770
- Bilal S, Rehman KU, Malik MY (2017) Numerical investigation of thermally stratified Williamson fluid flow over a cylindrical surface via Keller box method. *Results Phys* 7:690–696
- Rehman KU, Malik MY, Salahuddin T, Naseer M (2016) Dual stratified mixed convection flow of Eyring–Powell fluid over an inclined stretching cylinder with heat generation/absorption effect. *AIP Adv* 6(7):075112
- Ibrahim W, Makinde OD (2013) The effect of double stratification on boundary-layer flow and heat transfer of nanofluid over a vertical plate. *Comput Fluids* 86:433–441
- Abbasi FM, Shehzad TSA, Hayat MS Alhuthali (2016) Mixed convection flow of Jeffrey nanofluid with thermal radiation and double stratification. *J Hydrodyn Ser B* 28(5):840–849
- Makinde OD, Khan WA, Khan ZH (2013) Buoyancy effects on MHD stagnation point flow and heat transfer of a nanofluid past a convectively heated stretching/shrinking sheet. *Int J Heat Mass Transfer* 62:526–533
- Srinivasacharya D, Upendar M (2013) Effect of double stratification on MHD free convection in a micropolar fluid. *J Egypt Math Soc* 21(3):370–378
- Khanb I, Ullah S, Malika MY, Hussain A (2018) Numerical analysis of MHD Carreau fluid flow over a stretching cylinder with homogenous heterogeneous reactions. *Results Phys* 9(2018):1141–1147
- Prasad PD, Raju CSK, Varma SVK, Shehzad SA, Madaki AG (2018) Cross diffusion and multiple slips on MHD Carreau fluid in a suspension of microorganisms over a variable thickness sheet. *J Brazil Soc Mech Sci Eng* 40:256
- Balla CS, Kishan N, Gorla RSR, Gireesha BJ (2017) MHD boundary layer flow and heat transfer in an inclined porous square cavity filled with nanofluids. *Ain Shams Eng J* 8(2):237–254
- Raju CSK, Saleem S, Mamatha SU, Hussain I (2018) Heat and mass transport phenomena of radiated slender body of three revolutions with saturated porous: buongiorno's model. *Int J Therm Sci* 132:309–315
- Hayat T, Hussain Z, Alsaedi A, Farooq M (2016) Magneto hydrodynamic flow by a stretching cylinder with Newtonian heating and homogeneous-heterogeneous reactions. *PloS One*. <https://doi.org/10.1371/journal.pone.0156955>
- Rehman KU, Qaiser A, Malik MY, Ali U (2017) Numerical communication for MHD thermally stratified dual convection flow of Casson fluid yields by stretching cylinder. *Chin J Phys* 55(4):1605–1614
- Kishan N, Kavitha P (2013) Quasi linearization approach to MHD heat transfer to non-newtonian power-law fluids flowing over a wedge with heat source/sink in the presence of viscous dissipation. *IJMCAR* 3:15–28
- Madhu M, Kishan N (2015) Magnetohydrodynamic mixed convection stagnation-point flow of a power-law non-Newtonian nanofluid towards a stretching surface with radiation and heat source/sink. *J Fluids* 2015:14
- Dessie H, Kishan N (2014) MHD effects on heat transfer over stretching sheet embedded in porous medium with variable viscosity, viscous dissipation and heat source/sink. *Ain Shams Eng J* 5:967–977
- Salahuddin T, Malik Arif Hussain MY, Bilal S, Awais M (2016) MHD flow of Cattaneo–Christov heat flux model for Williamson fluid over a stretching sheet with variable thickness using numerical approach. *J Magn Magn Mater* 401:991–997
- Balasubramanian S, HariNarayanaRao B, Raju CSK (2019) Natural nonlinear convection of dusty fluid in a suspension of multi-wall carbon nanotubes nanoparticles with different temperature of water and suction. *SN Appl Sci* 1(6):642

27. Nadeem S, Khan M, Khan AU (2019) MHD oblique stagnation point flow of nanofluid over an oscillatory stretching/shrinking sheet: existence of dual solutions. *Phys Scr* 94(7):075204
28. Raju CSK, Mamatha SU, Rajadurai P, Khan I (2019) Nonlinear mixed thermal convective flow over a rotating disk in suspension of magnesium oxide nanoparticles with water and EG. *Eur Phys J Plus* 134(5):196
29. Mahmood Rashid, Bilal S, Majeed Afraz Hussain, Khan Ilyas, El-Sayed Sherif M (2019) A comparative analysis of flow features of Newtonian and power law material A New configuration. *J Mater Res Technol*. <https://doi.org/10.1016/j.jmrt.2019.12.030>
30. Nadeem S, RiazKhan M, Khan AU (2019) MHD stagnation point flow of viscous nanofluid over a curved surface. *Phys Scr* 94:11
31. Mamatha SU, Raju CSK, Shehzad SA, Abbasi FM (2018) Flow of Eyring-Powell dusty fluid in a deferment of aluminum and ferrous oxide nanoparticles with Cattaneo–Christov heat flux. *Powder Technol* 340:68–76
32. Bilal S, Majeed AH, Mahmood R, Khan I, Seikh AH, Sherif ESM (2020) Heat and mass transfer in hydromagnetic second-grade fluid past a porous inclined cylinder under the effects of thermal dissipation. *Diffu Radiat Heat Flux Energies* 13:278
33. Li X, Khan AU, Khan MR, Nadeem S, Khan SU (2019) Oblique stagnation point flow of nanofluids over stretching/shrinking sheet with Cattaneo–Christov heat flux model: existence of dual solution. *Symmetry* 11(9):1070
34. Raju CSK, Saleem S, Al-Qarni MM, Upadhya SM (2019) Unsteady nonlinear convection on Eyring–Powell radiated flow with suspended graphene and dust particles. *Microsyst Technol* 25(4):1321–1331
35. Awais M, Malik MY, Bilal S, Salahuddin T, Hussain A (2017) Magnetohydrodynamic (MHD) flow of Sisko fluid near the axisymmetric stagnation point towards a stretching cylinder. *Results Phys* 7:49–56
36. Khan MR, Pan K, Khan AU, Nadeem S (2020) Dual solutions for mixed convection flow of hybrid nanofluid near the stagnation point over a curved surface. *Phys A Statist Mech Appl* 1:1. <https://doi.org/10.1016/j.physa.2019.123959>

Publisher's Note Springer Nature remains neutral with regard to jurisdictional claims in published maps and institutional affiliations.